

## A Novel Electrochemical Biosensor Design and Fabrication

E. Basheer<sup>1</sup>, H. Bari<sup>1</sup>, C.F. Chin<sup>2</sup> and S. Nudra<sup>1</sup>

<sup>1</sup>Centre of Excellence for Advanced Research in Fluid Flow (CARIFF)

Universiti Malaysia Pahang, 26300 Gambang, Pahang, Malaysia.

<sup>2</sup>Faculty of Chemical and Natural Resources Engineering, Universiti Malaysia Pahang,  
26300 Gambang Pahang, Malaysia.

(Received: 10 September 2015; accepted: 14 November 2015)

Microfluidic Electrochemical biosensors become more desirable since it offered an attractive replacement for the bulky and expensive analytical instruments. The design and fabrication of such sensor with high quality and optimum effective surface area is of primarily importance for more accurate result. The biosensor was designed with two different chips; the microfluidic chip which was fabricated using PDMS (Polydimethylsiloxane) and the other chip of the biosensor was fabricated using glass substrate. The microfluidic chip has the dimension of 6mm in length and 4mm width. Built-in 8 microchannels with the variation in size from 100 to 1000  $\mu\text{m}$  was developed at the surface of it with inlets and outlets at the ends of each channel with the diameter of 1.5mm. An 8 electrode cells were developed at the center of each channel on a glass substrate. Each cell consisted of three electrodes, working electrode (WE), counter electrode (CE) and reference electrode (RE) with size of 100  $\mu\text{m}$ , 600  $\mu\text{m}$  and 600  $\mu\text{m}$  respectively. The surface quality of the fabricated chips was analyzed using scan electron microscope (SEM). There wasn't any deformation found in the wall of the channels. Moreover, the electrodes surface was of high resolution which will result in lower electrical noise during the application. A range of channels sizes was simulated using COMSOL Multiphysics simulation software. The optimal channel size was with width of 700 and depreciation on the current respond at higher sizes was observed. To this end, the fabricated sensor was desirable for the high performance of microbiological detection applications.

**Key words:** Microfluidics, Electrochemical Biosensor, Microscope, Microchannel.

---

With advancement in Biotechnology and diagnostic devices, biosensors have attracted the attention of researches<sup>1-5</sup>. Biosensors are various types; the most common type is the electrochemical biosensor. Electrochemical biosensors since the early of the last two decades have received higher attention from researchers and became more desirable since it offered an attractive replacement for the bulky and expensive analytical instruments<sup>6</sup>. In fact, electrochemical biosensors possess other advantage over the other types of biosensors; one of the most important advantages is that they can operate at ambient temperatures without the need

for external heating. Part from that, they can operate at very low power requirements and some are totally self-powered. However, electrochemical biosensor respond time and sensitivity are the major limitation of its type which usually caused by the diffusion limitation. The performance of the electrochemical biosensors is mainly depending on the diffusion of the analyte to the sensing surface which is the electrode surface in this case<sup>7</sup>. This usually the limiting step for detection step. To overcome this particular problem, different approaches have been presented in the past years. Meinhart *et al* were the earliest who use electrothermal stirring to improve the diffusion in the biosensor<sup>8</sup>. Squires *et al* has develop a model for the diffusion in microelectrode and microdetection cells which enclosed in microchannel<sup>9</sup>. Though, the model was

---

\* To whom all correspondence should be addressed.  
E-mail: esmail\_4230@yahoo.com

fund to be inapplicable for the unsteady state conditions. Kim & Zheng and Kim *et al* in their studies they numerically studied the analyte transport as a function of the position of a nanowire-based sensor inside a microchannel, stressing on the fact that the challenge for nanobiosensors is not the sensor itself but the fluidic system that delivers the sample<sup>10,11</sup>.

In our study we highlight a solution to this limitation, where we relate the design factor to this limitation and we optimized it for better performance.

### **Design and Study**

The design of the biosensor was done using AutoCAD software for the 2D drawing and SolidWorks software to draw the 3D drawing as shown in figure 1. The sensor was designed to have 8 integrated detection channels with external connections gold pads with width of 1mm for the electrical testing measurements. An additional separated connections pad at the entrance and the exits of each channel was designed to allow additional electrical field supply to the channel. The details of the design are presented in the next part. The cell electrodes includes three electrodes, working electrodes made of gold and carbon, counter electrode made of silver and lastly reference electrode made of AgCl/Cl<sub>2</sub>.

### **Microfluidic channels**

The microchannels or microfluidic channels in this design was varied in their size and dimension. There are eight channels, four pairs of channels, and each pair have the same high and width. The size of the channels play an important role in enhancing the ability of different constituent to flow throughout the channel as well have higher contact area with electrode surface. In pressure driven flow, flow is induced by a pressure gradient. The geometry of the channel and flow rates affects the nature of the flow. In our design we have consider these parameters in order to obtained better result<sup>12</sup>. The channels dimensions are described in table 1:

The size and shape of the cannels were chosen based on optimization options where the simulation result presented in this paper. The width of the channel was varied and the depth was fixed at 1000 μm.

The microfluidic channels in PDMS are constructed by a soft lithography technique. The

fabrication starts by preparing the silicon wafer pattern where it defined the shape of the channel. A photoresist was spin-coated into the prepared mold mask with thickness of 1000 μm. The master on the silicon wafer is then coated with tridecafluoro-1,1,2,2-tetrahydrooctyl-1-trichlorosilane in a desiccator under vacuum for 2 h to prevent irreversible bonding between the silicon and PDMS. A mixture of 8 cm<sup>3</sup> PDMS prepolymer and 0.8 cm<sup>3</sup> curing agent is degassed under vacuum, poured over the master, and cured at 75°C for 1 h. after that the fabricated PDMS channel was peeled off and stored.

### **Electrochemical Chip (Electrodes Chip)**

The electrodes chip was designed to be varied in size and materials. This design is giving advantages in term of comparison and optimization of the two important parameters. The species has to be transported to the electrode surface in order to reacts and exchanges electrons with the electrode<sup>13</sup>. Rate of chemical reactions is dependent of the mass transport phenomena and the electrode kinetics. The size of the electrode has been varied for breaking the diffusion and electron conductivity barriers<sup>14</sup>. Two mean types of materials were used in this study, gold electrodes and carbon paste electrodes. The first type is more commonly used in electrochemical biosensors for its properties such as unreactive with other chemicals which will secure the process of getting contact with analyte. The proposed sizes of electrodes are presented in table 2.

There are 40 sets of electrodes chips and with similar distribution but the change in the size of the electrodes or the surface area of the electrodes as described in table 3.

Noticing that in table 3 each size of electrode is fabricated in two pairs, gold pair and the other one is carbon where the four different size of channels whith the respect to the electrode material type. Eight cells are fabricated in parallel on a glass substrate. The glass slide is first cleaned sequentially with acetone and isopropanol, dried with nitrogen, and baked on a hot plate at 110°C for 5 min. Positive photoresist (AZ 9245 Clariant Corp., Somerville, NJ) is used during the photolithography process to obtain an over-cut structure for the subsequent lift-off of electrodes, interconnection lines, and contact pads. Electron beam evaporation is performed to deposit 20 nm of

Ti as an adhesion layer and then a 300 nm Au electrode layer. After lift-off, we deposit a 500 nm Si<sub>3</sub>N<sub>4</sub> insulating layer using plasma-enhanced chemical vapor deposition (PECVD) operated at 900 mTorr. The feedstock gases contain NH<sub>3</sub> (2 sccm), N<sub>2</sub> (200 sccm), and SiH<sub>4</sub> (75 sccm). The deposition time is 15 min at 16 W rf power. The insulating layer is then patterned with positive photoresist (Microposit S1818, Shipley Company, Marlborough, MA) as an etching mask, then selectively etched using CF<sub>4</sub> plasma to expose active-area windows on the surfaces on the working electrodes, reference electrodes, counter electrodes, and contact pads. After removal of the etching mask, the positive photoresist AZ 9245 is again patterned for subsequent lift-off of metal. Electron beam evaporation is used to deposit 20 nm Ti and 1 μm Ag on the reference electrode areas. The Ag layer is converted into a Ag/AgCl stack by Cl<sub>2</sub> plasma treatment<sup>15</sup>. The plasma chamber pressure is set to 100 mTorr under the Cl<sub>2</sub> flow rate of 100 sccm for 120 s at 100 W rf power. The thickness of the AgCl layer is measured by soaking the substrate in concentrated NH<sub>3</sub>OH to dissolve the AgCl portion of the stack. The thickness of the AgCl layer is 0.8 μm and the thickness of the Ag layer is 0.7 μm. After plasma chlorination of silver, the photoresist is removed.

#### Chips Binding

Various bonding techniques have been reported for fabrication of polymer substrates, such as thermal bonding<sup>16</sup>, solvent bonding<sup>17</sup>, plasma oxidation<sup>18, 19</sup>, the use of adhesives<sup>20</sup>, UV/ozone surface treatment<sup>21</sup>, and laser welding<sup>20</sup>. A successful bonding process must preserve channel integrity, geometry, and structure, and offer high bonding strength. A modified high-density cross-linked polyethylene foam polymer adhesive was used to bind the two chips. The method was used to bind the chips consist of three steps. The chips were cleaned gently using acetate followed by adhesive application at room temperature. Finally, a low pressure 5 psi and temperature of 38 °C were applied on the bonded chips for 40 mins. In this method a combination of surface modification and adhesive application was used to bind the two chips, where the adhesive was used is of solvent resistance nature.

#### Microchannel Size Simulation

The size of microchannel as mentioned

earlier in this paper is affecting the diffusion limitation which in order affecting the sensor performance. The selection of the optimal size of channel will define the quality of the sensor respond to the target. In this study, we simulate a range of microchannels sizes for the glucose testing sensor using COMSOL Multiphysics software. The parameters used for this study are listed in table 4.

## RESULT AND DISCUSSION

### Simulation Result

The specific purpose of the simulations presented in this paper is to find the optimum microchannels dimensions and testing conditions for a glucose base biosensor. A simulate for the current respond at different dimensions of microchannels was carried out using COMSOL Software. The simulated biosensors were given the same parameters in the simulation entry as described in table 4.

The formation of current respond to the existence of the analyte target (glucose in this case) is direct proportional to the target concentration deposited to the surface of the electrode. Major concern at this point is given to the enhancement of the target deposition to the surface of the electrode. With increase in the target concentration at the surface of the electrode the respond or the average current produced is increased. Figure 3 shows the respond of the sensor to the target where the channel used was the width of 100 μm.

The relation between the current density and the actual cross sectional area of the channel is presented in equation 1.

$$I = \frac{\sigma AV}{L}$$

where  $\sigma$  is the measured bulk electrical conductivity,  $V$  is the supplied voltage,  $A$  is the cross sectional area of the channel, and  $L$  is the channel length from the nominal PDMS mold dimensions<sup>22</sup>.

This study shows that the current detected at the microelectrodes respond is limited by the diffusion of the charge species from the bulk of the solution to the electrode surface. At long times, the diffusion layer extends along the channel length direction, and the charge species

are depleted at the electrode surfaces. However, the increase of the channel size was dramatically enhancing the response as shown in figure 4, 5 and 6 where at channel width of 100  $\mu\text{m}$  the current

**Table 1.** Microfluidic Channels Dimension

Channel	Width ( $\mu\text{m}$ )	Material	Shape
1&2	100	PDMS	Rectangular
3 &4	400	PDMS	Rectangular
5& 6	700	PDMS	Rectangular
7& 8	1000	PDMS	Rectangular

**Table 2.** Microelectrodes Material and Size with Electrode size of 100 $\mu\text{m}$

Channel	Electrode Type	Electrode Size ( $\mu\text{m}$ )	Channel Size ( $\mu\text{m}$ )
1	Gold	100	100
2	Carbon	100	100
3	Gold	100	400
4	Carbon	100	400
5	Gold	100	700
6	Carbon	100	700
7	Gold	100	1000
8	Carbon	100	1000

**Table 3.** Sets Distribution

Electrode Type set	Electrode Size	Number of Chips ( $\mu\text{m}$ ) produced
Gold	10	4
Carbon	10	4
Gold	20	4
Carbon	20	4
Gold	40	4
Carbon	40	4
Gold	70	4
Carbon	70	4
Gold	100	4
Carbon	100	4

**Table 4.** Simulation parameters.

Name	Expression	Value	Description
c_glucose_ext	5[ $\mu\text{mol/L}$ ]	0.005 mol/ $\text{m}^3$	External glucose concentration
c_ferro_ext	1[ $\mu\text{mol/L}$ ]	0.001 mol/ $\text{m}^3$	Ferrocyanide concentration
c_ferri_ext	50[mmol/L]	50 mol/ $\text{m}^3$	Ferricyanide concentration
V_max	1.5e-5[mol/L/s]	0.015 mol/( $\text{m}^3 \cdot \text{s}$ )	Maximum rate of reaction
Km	0.5[mmol/L]	0.5 mol/ $\text{m}^3$	Michaelis-Menten constant

density was 0.075 and was increase to reach to 0.48 at channel width of 700  $\mu\text{m}$ . This can be explained as the increase of the channel width has increased the chances for more targets to bind to the electrode surface which consequently making more free electrons in the solution which will increase the current density<sup>22</sup>. However, with increase in the channel size it appears to decrease the current density of the product current. This can be explained as the change from the diffusion-limit currents to the product deposition limit at the surface of the electrode where the increase in the bulk volume. The attraction of the electrodes to the migrant charges in the bulk solution will increase with increase in the volume. However, at low volumes the attraction force is wake. Therefore, less product ions will be deposited at the electrode surface. As shown in figure 7 using channel size of 1000 the current density is decreased compare to the channel size of 700.

#### Fabricated chip surface analysis

After fabricating the microchip, the quality of the fabricated channel surface has been analyzed. Concerning about the quality of fabrication, several factors have been studied which affect the rate of reaction and the quality of translating the reaction into signal<sup>13</sup>. These factors are the rate of the electron transfer at the electrode surface, the mass transfer rate at the electroactive bulk, the side chemical reactions which may result in forming an isolation layer or deactivation of the electrode and surface properties. For instant, the rate of electrons transfer is depending mainly on the type of electrodes materials.

The following figure shows the microscopic picture of the surface of the microchannel. As shown in figure 5c the surface of microchannel is a smooth and uniform in texture. This smoothness will reduce the share stress to the fluid, which in order will reduce diffusion layer at the surface of the channel.



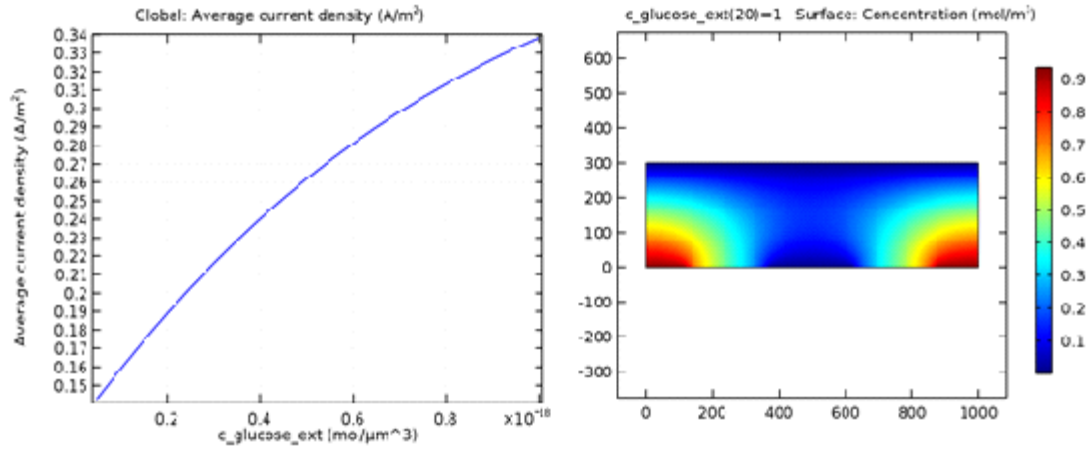


Fig. 4: Simulation Result for the Global Average Current Density ( $A/m^2$ ) for the  $300 \mu m$  Channel size

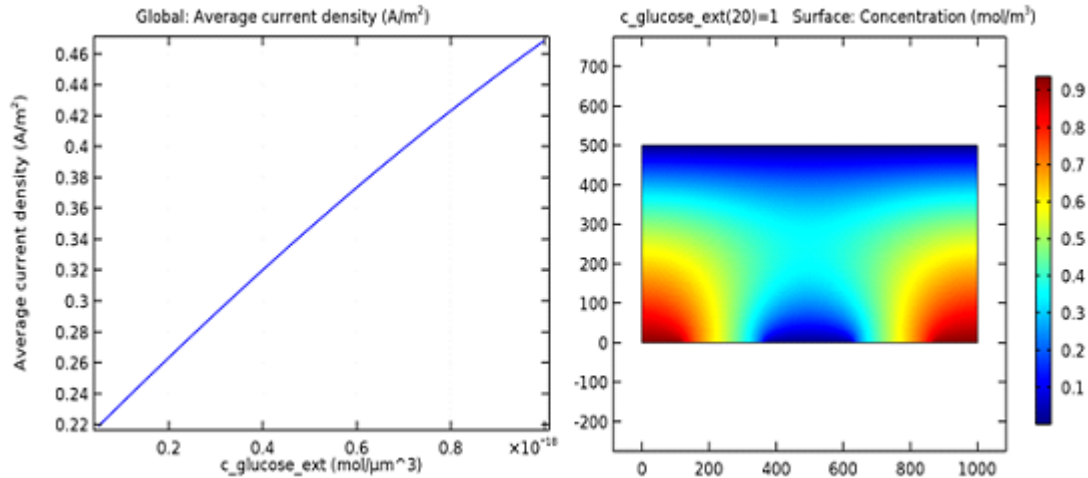


Fig. 5: Simulation Result for the Global Average Current Density ( $A/m^2$ ) for the  $500 \mu m$  Channel size

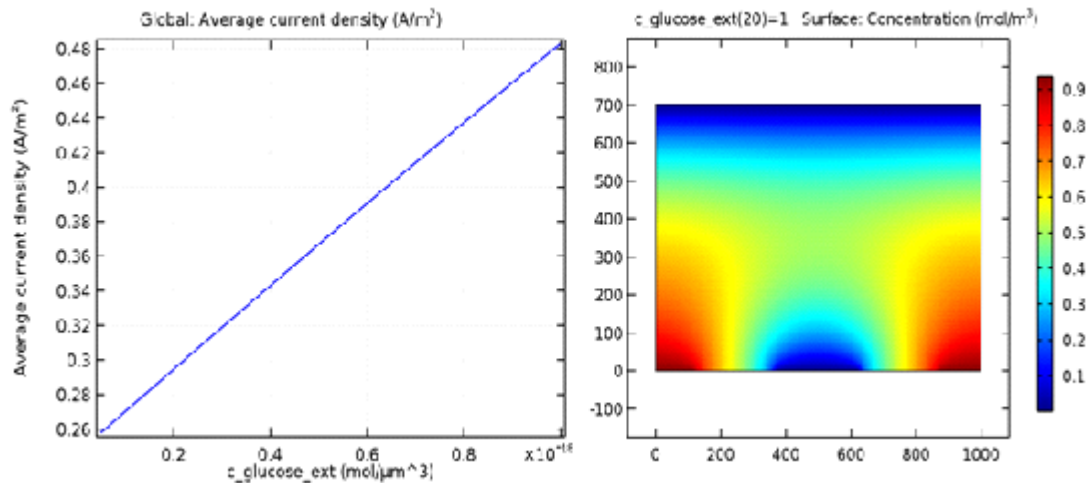


Fig. 6: Simulation Result for the Global Average Current Density ( $A/m^2$ ) for the  $700 \mu m$  Channel size

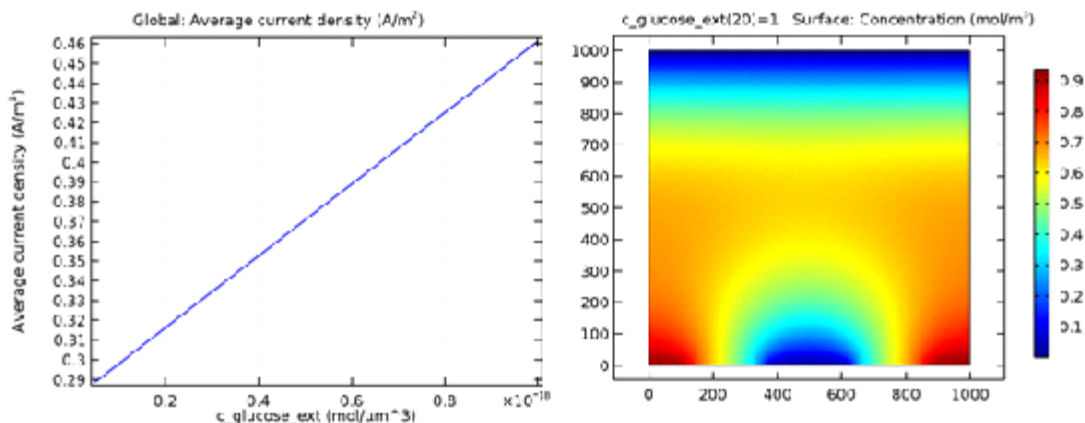


Fig. 7. Simulation Result for the Global Average Current Density (A/m<sup>2</sup>) for the 1000 μm Channel size

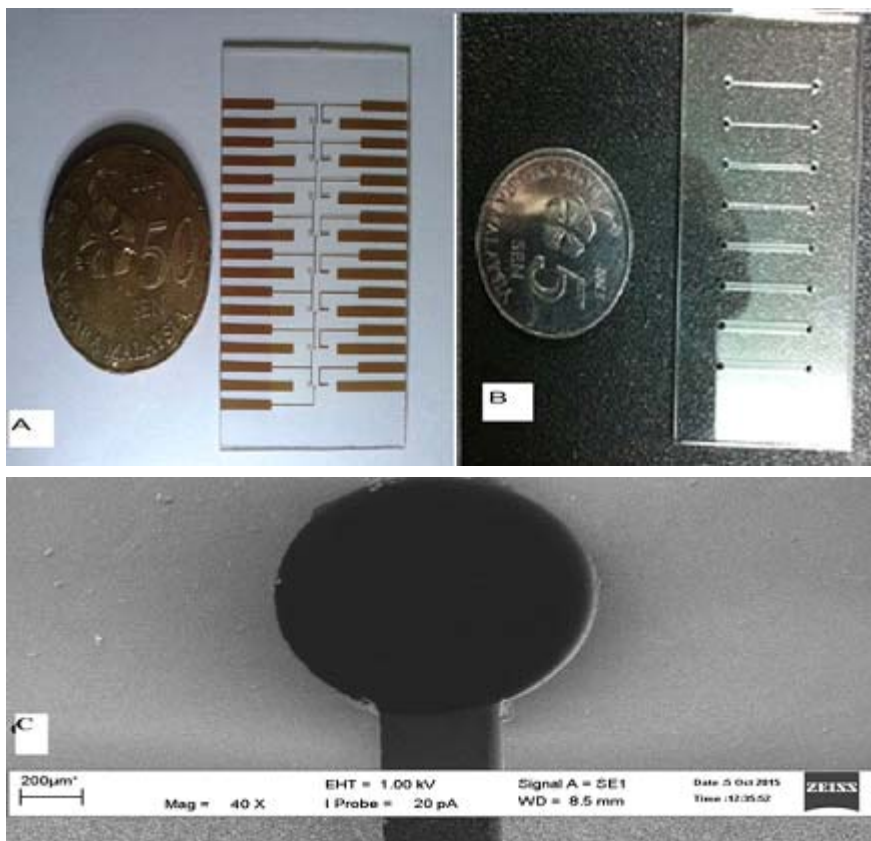


Fig. 5. (a) The Fabricated Electrochemical Biosensor Complete Chip. B) The Microchannels Chip consist of 8 parallel channels C) SEM capture of the inlet of the microchip channel

**CONCLUSION**

An electrochemical biosensor was designed, simulated and fabricated. A total of 40 sets of chips were fabricated where the variation was in the channel size, electrode size and electrode

materials. The design has been justified and investigated using COMSOL Multiphysics simulation software. The simulation result showed and proportional relation between the channels size and the respond of the sensor. SEM image showed no deformation in the wall of the channels.

## REFERENCES

- Hamidi-Asl, E., *et al.*, A review on the electrochemical biosensors for determination of microRNAs. *Talanta*, 2013, **115**(0): p. 74-83.
- Vidal, J.C., *et al.*, Electrochemical affinity biosensors for detection of mycotoxins: A review. *Biosensors and Bioelectronics*, 2013; **49**(0): 146-158.
- Prieto-Simón, B., *et al.*, Electrochemical biosensors as a tool for antioxidant capacity assessment. *Sensors and Actuators B: Chemical*, 2008; **129**(1): 459-466.
- Wang, J., Electrochemical biosensors: Towards point-of-care cancer diagnostics. *Biosensors and Bioelectronics*, 2006; **21**(10): p. 1887-1892.
- Ikeda, T. and K. Kano, An electrochemical approach to the studies of biological redox reactions and their applications to biosensors, bioreactors, and biofuel cells. *Journal of Bioscience and Bioengineering*, 2001; **92**(1): p. 9-18.
- Jena, B.K. and C.R. Raj, Electrochemical biosensor based on integrated assembly of dehydrogenase enzymes and gold nanoparticles. *Analytical chemistry*, 2006; **78**(18): 6332-6339.
- Shilton, R., *et al.*, Particle concentration and mixing in microdrops driven by focused surface acoustic waves. *Journal of Applied Physics*, 2008; **104**(1): p. 014910.
- Sigurdson, M., D. Wang, and C.D. Meinhart, Electrothermal stirring for heterogeneous immunoassays. *Lab on a Chip*, 2005; **5**(12): 1366-1373.
- Squires, T.M., R.J. Messinger, and S.R. Manalis, Making it stick: convection, reaction and diffusion in surface-based biosensors. *Nature biotechnology*, 2008; **26**(4): p. 417-426.
- Kim, J., *et al.*, Applications, techniques, and microfluidic interfacing for nanoscale biosensing. *Microfluidics and Nanofluidics*, 2009; **7**(2): 149-167.
- Kim, D.R. and X. Zheng, Numerical characterization and optimization of the microfluidics for nanowire biosensors. *Nano letters*, 2008. **8**(10): p. 3233-3237.
- Noh, H.-S., *et al.*, Microstructural factors of electrodes affecting the performance of anode-supported thin film yttria-stabilized zirconia electrolyte (<math>\lambda</math>) solid oxide fuel cells. *Journal of Power Sources*, 2011; **196**(17): p. 7169-7174.
- Oyama, N. and F.C. Anson, Factors Affecting the Electrochemical Responses of Metal Complexes at Pyrolytic Graphite Electrodes Coated with Films of Poly (4 Vinylpyridine). *Journal of The Electrochemical Society*, 1980; **127**(3): p. 640-647.
- Wu, C., *et al.*, Recent advances in taste cell- and receptor-based biosensors. *Sensors and Actuators B: Chemical*, 2014. **201**(0): p. 75-85.
- Liu, S. and H. Ju, Reagentless glucose biosensor based on direct electron transfer of glucose oxidase immobilized on colloidal gold modified carbon paste electrode. *Biosensors and Bioelectronics*, 2003; **19**(3): p. 177-183.
- Kim, D.S., *et al.*, Collapse-free thermal bonding technique for large area microchambers in plastic lab-on-a-chip applications. *Microsystem Technologies*, 2008; **14**(2): 179-184.
- Koesdjojo, M.T., C.R. Koch, and V.T. Remcho, Technique for microfabrication of polymeric-based microchips from an SU-8 master with temperature-assisted vaporized organic solvent bonding. *Analytical chemistry*, 2009; **81**(4): 1652-1659.
- Chen, W. and T.J. McCarthy, Chemical surface modification of poly (ethylene terephthalate). *Macromolecules*, 1998; **31**(11): 3648-3655.
- Hao, Z., *et al.*, Modification of amorphous poly (ethylene terephthalate) surface by UV light and plasma for fabrication of an electrophoresis chip with an integrated gold microelectrode. *Journal of Chromatography A*, 2008; **1209**(1): 246-252.
- Ussing, T., *et al.*, Micro laser welding of polymer microstructures using low power laser diodes. *The International Journal of Advanced Manufacturing Technology*, 2007; **33**(1-2): 198-205.
- Tsao, C., *et al.*, Low temperature bonding of PMMA and COC microfluidic substrates using UV/ozone surface treatment. *Lab on a Chip*, 2007; **7**(4): 499-505.
- Godwin, L.A., *et al.*, Measurement of microchannel fluidic resistance with a standard voltage meter. *Analytica chimica acta*, 2013; **758**: 101-107.